DEFORMATION BEHAVIOR AND FRACTURE MECHANISMS OF ROCKS

T. K. Lew

Naval Civil Engineering Laboratory

Prepared for:

Defense Nuclear Agency

May 1973

DNA 13.018

Technical Report

R 788

Sponsored by

DEFENSE NUCLEAR AGENCY

May 1973

NAVAL CIVIL ENGINEERING LABORATORY
Port Hueneme, California 93043

DEFORMATION BEHAVIOR AND FRACTURE MECHANISMS OF ROCKS

By

T. K. Lew

DEFORMATION BEHAVIOR AND FRACTURE MECHANISMS OF ROCKS

Technical Report R-788

Y-F008-08-02-108, DNA 13.018

by

T. K. Lew

ABSTRACT

A study was conducted to determine from the literature what is known about the deformation behavior and fracture mechanisms of intact, fractured, and jointed rocks. The literature indicates the following: The mechanical properties of an intact rock are not unique; rather, they vary with mineral composition, grain size, state of stress, and strain rate. Deformation behavior and fracture mechanisms of an intact rock are characterized by crack growth and deformation of the constituent grains. Dilatancy of an intact rock under compression is associated with shear stress. Fractured rock can still carry load. Deformation of a fractured rock tends to concentrate along the major discontinuities. Furthermore, deformation of a jointed material is characterized by slip along joints, interlocking of the intact blocks, and fracturing of the intact blocks. Under a given state of stress, the stiffness and the strength of a fractured or jointed rock are generally lower than those for the intact rock.

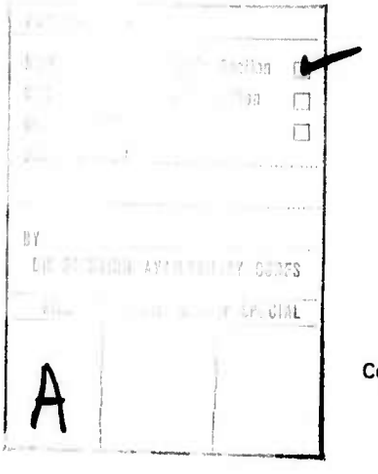

CONTENTS

Unclassified
Security Classification

DOCUMENT CONTROL DATA - R & D

Security classification of title, body of abstract and indexing annotation must be entered when the overall report is classified)

1 ORIGINATING ACTIVITY (Corporate author) Naval Civil Engineering Laboratory Port Hueneme, California 93043	2a. REPORT SECURITY CLASSIFICATION Unclassified 2b GROUP

3 REPORT TITLE

DEFORMATION BEHAVIOR AND FRACTURE MECHANISMS OF ROCKS

4 DESCRIPTIVE NOTES (Type of report and inclusive dates)
Not final; March 1972 – July 1972

5 AUTHOR(S) (First name, middle initial, last name)

T. K. Lew

6 REPORT DATE May 1973	7a. TOTAL NO OF PAGES 47 41	7b. NO OF REFS 36
8a CONTRACT OR GRANT NO b PROJECT NO Y-F008-08-02-108 c d	9a. ORIGINATOR'S REPORT NUMBER(S) TR-788 9b. OTHER REPORT NO(S) (Any other numbers that may be assigned this report)	

10 DISTRIBUTION STATEMENT

Approved for public release; distribution unlimited.

11 SUPPLEMENTARY NOTES	12 SPONSORING MILITARY ACTIVITY Defense Nuclear Agency Washington, D. C. 20305

13 ABSTRACT

A study was conducted to determine from the literature what is known about the deformation behavior and fracture mechanisms of intact, fractured, and jointed rocks. The literature indicates the following: The mechanical properties of an intact rock are not unique; rather, they vary with mineral composition, grain size, state of stress, and strain rate. Deformation behavior and fracture mechanisms of an intact rock are characterized by crack growth and deformation of the constituent grains. Dilatancy of an intact rock under compression is associated with shear stress. Fractured rock can still carry load. Deformation of a fractured rock tends to concentrate along the major discontinuities. Furthermore, deformation of a jointed material is characterized by slip along joints, interlocking of the intact blocks, and fracturing of the intact blocks. Under a given state of stress, the stiffness and the strength of a fractured or jointed rock are generally lower than those for the intact rock.

DD FORM 1 NOV 65 1473 (PAGE 1)
S/N 0101-807-6801

Unclassified
Security Classification

14 KEY WORDS	LINK A		LINK B		LINK C	
	ROLE	WT	ROLE	WT	ROLE	WT
Intact rock						
Fractured rock						
Jointed rock						
Deformation						
Fracture						
Mineral composition						
Grain size						
Stress						
Strain						
Crack growth						
Dilatancy						
Asperities						
Strength						
Stiffness						
Friction						
Mohr envelope						
Compression						

INTRODUCTION

Purpose

The purpose of this study is (1) to discover from the literature what is known about the deformation behavior and fracture mechanisms of intact, fractured, and jointed rock, and (2) to evaluate quantitatively the parameters that determine the deformability and strength of rock in the field. The ultimate goal of the effort is to incorporate this knowledge into the development of nonlinear finite element computer programs for calculating the behavior of lined or unlined cavities in rock from static or blast loads, and to utilize the knowledge in developing methods for rock fragmentation. This study was sponsored by the Defense Nuclear Agency.

Background

The mechanical properties of a given type of natural rock are highly variable from site to site, and often from one location to another within a given site. These properties are dependent on the mineral composition of the rock, its grain size, grain geometry, the existing state of stress, and strain rate. Natural rock masses are generally not homogeneous, but contain discontinuities, such as joints and faults, that have a significant influence on their behavior. Furthermore, rock surrounding an underground opening is often fractured during the excavation process. Deformation of a rock mass under load tends to concentrate along these discontinuities. Observations in the field and in laboratory experiments indicate that the stability of an opening in a rock field is governed by the larger discontinuities in the vicinity of the opening.[1-3] Thus, a complete understanding of the behavior of jointed and fractured rock is a prerequisite for computing the behavior of lined or unlined openings in a rock mass from static or dynamic loads. First, however, a good knowledge of the behavior of intact rock is necessary.

The following definitions are presented to facilitate future discussions. An intact rock is a continuous rock body on a macroscopic scale; however, it may contain discontinuities on a microscopic scale. Basically, no clear distinction exists between fractured rock and jointed rock because both contain

discontinuities in the form of fractures. In this study, however, a fractured rock is defined as a rock mass with a large number of discontinuities whose location, lengths, and orientations are not well known. On the other hand, a jointed rock is defined as a discontinuous rock mass with well known discontinuity geometries such as joint location, length, and orientation.

Analysis of the Problem

Three possible alternatives for analyzing the behavior of rock surrounding an opening during and after excavation, and for determining the survivability of a lined or unlined opening in rock from imposed loading are full-scale testing, laboratory model testing, and analytical modeling.

Useful performance data on a prototype rock–structure system can be obtained from full-scale tests. However, full-scale tests are expensive and the number of measurements obtainable is limited by economic considerations. In addition, extrapolation of the prototype test results from one site to another is difficult, particularly in cases where discontinuities in the rock dominate the behavior.

Laboratory model tests are more economical than full-scale testing, but are still expensive. Parameters that have significant influence on a model may be controlled by the experimenter. However, modeling natural rocks is difficult because their deformation behavior is not unique. It follows that scaling of laboratory test results to prototype behavior is almost impossible. Nonetheless, laboratory model tests are useful for observing and studying probable modes of failure of a rock mass or an opening in rock. They also provide good checks on solutions from analytical models because significant parameters influencing the response of a model may be controlled in laboratory experiments.

Most analytical models are of limited utility because they do not accurately characterize the material properties, system geometry, and boundary conditions. The finite element method permits a better characterization than other methods.[4] It can be used to analyze problems with both material and geometric nonlinearity, such as lined or unlined openings in a rock mass subjected to static or dynamic loads. In principle, this method will permit the analysis of structures with arbitrary geometry and boundary conditions and with discontinuities, such as joints and faults.[5-7]

At present, however, accurate analysis of the behavior of openings in a rock mass awaits further improvements in the model. Once developed, the finite element method is expected to provide an economical means for analyzing the behavior of openings in rock masses under different loading conditions.

One of the main barriers to further development of the finite element method for analyzing structures built in rock is the lack of knowledge about the deformation behavior and failure mechanisms of rock masses. Considerable work is underway to improve the state of knowledge, as is indicated in subsequent sections of this report.

INTACT ROCK

A basic understanding of the deformation behavior and fracture mechanisms of intact rock is fundamental to comprehending the behavior of fractured rock and jointed rock. The properties of a given rock vary with its mineral composition, grain size, state of stress, water content, and other factors. As a consequence, no universally reliable theory for predicting rock behavior exists.

Deformation Behavior in Compression

A rock may be classified as a brittle or a ductile material according to its stress-deformation characteristics.* Most rocks are classified as brittle materials at room temperature and relatively low confining pressures. However, a brittle rock may behave in a ductile manner under a different set of conditions. Limestone, for example, behaves in a brittle manner at room temperature and zero confining pressure, but in a ductile manner at relatively high confining pressures and/or temperatures.

Recent progress in research on the deformation behavior of rock can be found in the studies by Brace and Byerlee[8] and by Bieniawski.[9] Most of the experimental studies by the different investigators deal with brittle materials. Significantly, the findings of Brace, Paulding, and Scholz[10] indicate that the same mechanisms may occur in both ductile and brittle materials. Internal deformation and fracture mechanisms of an intact rock are characterized by crack growth and the deformation of the constituent mineral grains. The stages of deformation for intact rock in compression and internal mechanisms related to the stress–strain behavior are presented in Figure 1. The four stages of deformation are:

1. Closing of pre-existing cracks
2. Perfectly elastic deformation

* A brittle material is one that exhibits little or no plastic deformation before rupture; a ductile material is one that exhibits considerable plastic deformation before rupture.

3. Stable fracture propagation

4. Unstable fracture propagation

On a microscopic scale, intact rock is not homogeneous, but contains pre-existing cracks, randomly distributed among the mineral grain boundaries. These cracks close under small compressive loads, resulting in the nonlinear axial stress-axial, -lateral, and -volumetric strain curves shown in range 1 of Figure 1. In this range, deformation of the mineral grains contributes very little to the overall deformation of the specimen. Conclusion of the crack closure process is marked by the crack closure point. The length of the stress–strain curve attributed to crack closure is rather short for a low porosity rock, such as granite, but is fairly long for a porous rock, such as sandstone. Load increments above the crack closure point cause the rock specimen to deform in an elastic manner, as characterized by the linear stress–strain curves shown in Figure 1. Deformation of the specimen at this stage is caused by deformation of the mineral grains. Fracture initiation, manifested by a departure from linearity of the axial stress-volumetric and -lateral strain curves, is the stress level at which one or more of the pre-existing cracks start to extend. It marks the end of elastic deformation and the beginning of stable fracture propagation—the failure process by which cracks in the rock are extended.

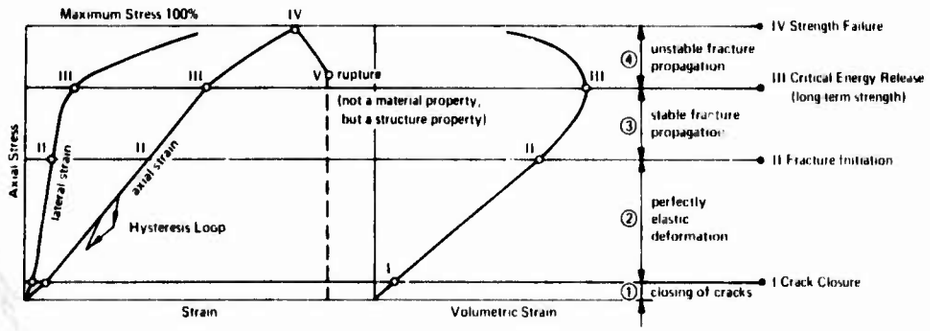

Figure 1. Internal mechanism related to the stress–strain behavior (after Bieniawski[9]).

During stable crack propagation, crack extension is a function of loading and can be controlled accordingly. Fracture initiation does not lead to the immediate failure of the rock. Furthermore, fracture propagation ceases if the load is held constant. The critical energy release point marks the end of the stable propagation region. This point is characterized by the deviation from linearity of the axial stress–axial strain curve and the knee of the axial stress–volumetric strain curve (Figure 1). Incidentally, Bieniawski[9] found that the stress at the critical energy release point corresponds to the long-term strength of the rock.

Unstable fracture propagation commences at loads above the critical energy release point. Above the critical energy release point, crack extension becomes uncontrollable. Crack extension is now governed by the crack propagation velocity and the energy stored in the rock. According to Bieniawski, fracture propagation will eventually cease if the load is held constant.[11] The predominant direction of both stable and unstable crack propagation is parallel to the direction of maximum principal compressive stress. This has been confirmed by microscopic examination of specimens in which stable and unstable fracture propagation has taken place.[9] In the unstable region, the rock becomes dilatant with increasing load; that is, the volume of the specimen increases with increasing compressive stress. This bulking behavior is due to the opening of cracks in the axial direction.[12, 13] During bulking, the volume increase of a cylindrical rock specimen due to radial expansion is greater than the volume reduction due to compression in the axial direction. Apparently, the rock behaves as an anisotropic material when it becomes dilatant.

Bulking of the surrounding rock under load may cause a tunnel liner to collapse if the liner is not designed for the loading associated with bulking. This type of failure occurred in the Pile Driver event.[2] Fortunately, an estimate of the stress induced on the liner because of bulking may be obtained from laboratory tests. Radial expansion of a cylindrical rock specimen under a given compressive axial stress, σ_1, is eliminated in one-dimensional strain tests by applying a confining pressure, σ_3. Experimental results indicate that a unique relation exists between σ_1 and σ_3 for each rock. An estimate of the stress due to bulking in a field situation can be obtained from the one-dimensional strain test. This load is equal to σ_3, the confining pressure in the one-dimensional strain test, corresponding to the strength failure (maximum strength) obtained in a triaxial test.

The tangent modulus of elasticity of the rock decreases rapidly with increasing load in the unstable fracture propagation region because of the advanced cracking taking place in the rock. The rock structure is damaged considerably by the shattering of the grains, a phenomenon which is not observed in stable crack propagation. Furthermore, the fracture propagation velocity increases with load in the unstable region and attains a terminal value coinciding with strength failure (Figure 1).

Strength failure, a characteristic property of the rock, corresponds to the maximum strength of the material. That is, the fracture process is concluded when strength failure is reached. Strength failure defines the transition from a predominantly continuous material (rock material) to a predominantly discontinuous material (rock system). After strength failure, the cracks coalesce and forking takes place, leading to ultimate rupture.

Rupture is the fracture process associated with the rock system when complete separation of the material takes place, rendering the rock system (structure) useless. Rupture is not a fundamental property of the material, but one of the rock system. It defines the stability of the fractured rock structure.

Surprisingly, a rock specimen can still carry load in a predictable manner after strength failure although it has been fractured.[11] The strength of the fractured rock, however, decreases with increasing deformation. Field observations show that rock adjacent to an opening is generally fractured during the excavation process as a result of blasting or stress relief; yet, this fractured rock is still able to carry load. The practical implication from the above observations is that an opening in rock can remain stable even if a portion of the rock in the vicinity of the opening has reached its strength failure. Strength failure of the rock, therefore, should not govern the design of an opening in rock. Instead, the stability of the structural system (the opening plus the surrounding rock mass) should govern the design. The shape and layout of the opening should be chosen to obtain a stable structure that will not fail if the rock material surrounding the opening has reached its maximum strength.

Hysteresis and permanent strains are exhibited in the dilatation and the shear curves during unloading and reloading (Figures 2 and 3). The unloading and reloading portions of the mean stress–volumetric strain curves are approximately parallel to the hydrostat (Figure 2). On the other hand, the reloading in the shear stress–strain curve (Figure 3) is approximately parallel to the previous unloading path. Once the previous maximum shear stress is reached on reloading, the curve resumes as before.

The deformation behavior and fracture mechanisms of rock in tension are similar to those under compression with the following exceptions:

1. Crack closure is generally absent.
2. The stages of stable and unstable fracture propagation are very short in duration because a crack propagates in its own plane.

For example, fracture initiation for norite, an igneous rock, takes place in compression at about 38% of the maximum load, while fracture initiation in tension is at 94.5% of the maximum load. Furthermore, unstable fracture propagation begins in compression at 73.0% and in tension at 96.5% of the maximum load. Thus, for practical purposes, fracture initiation and strength failure in tension may be assumed to occur almost simultaneously, with the process of fracture propagation almost nonexistent.

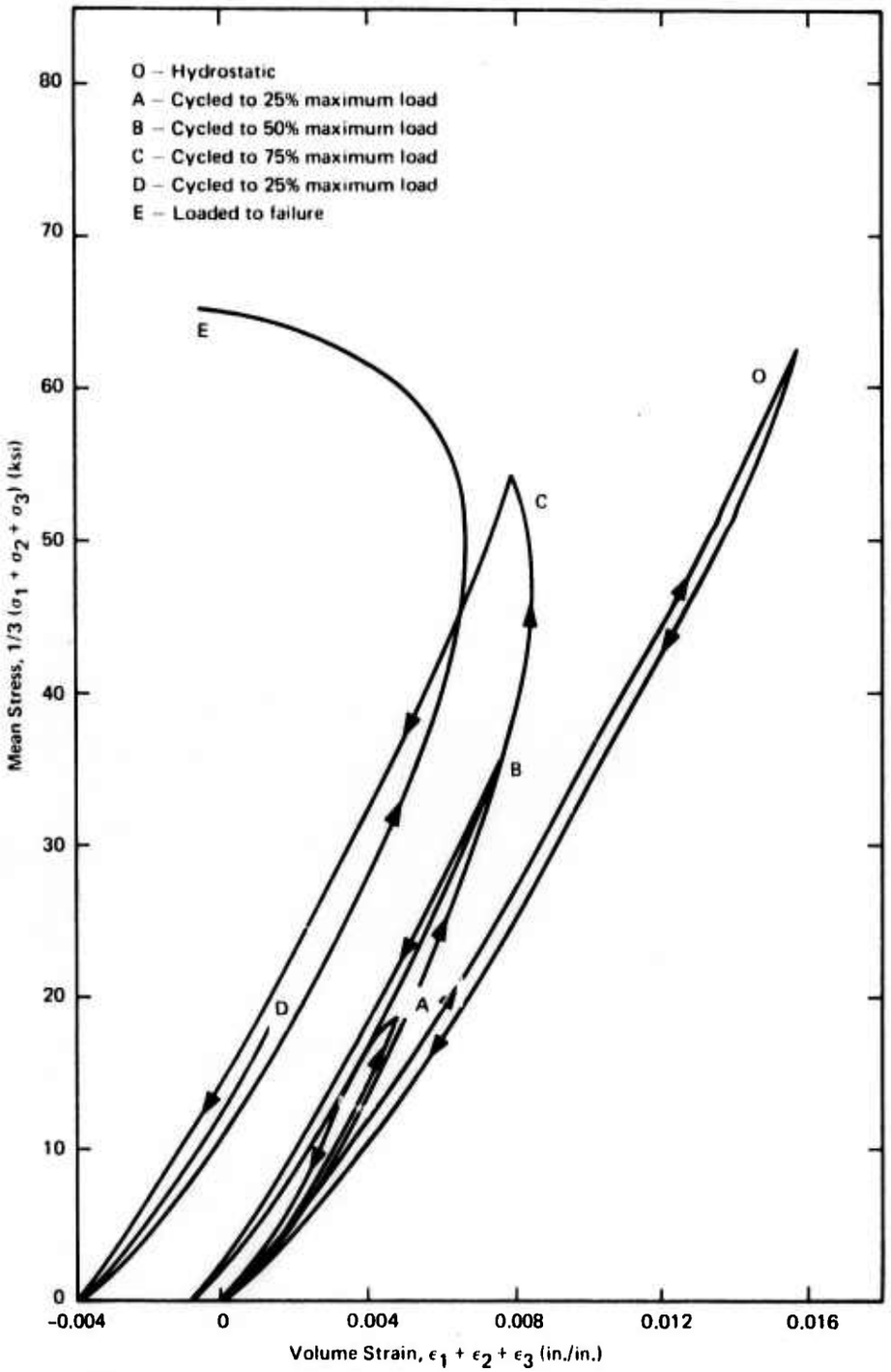

Figure 2. Dilatation stress–strain curves for Cedar City 6-inch-core granite, specimen no. 18, with $\sigma_3/\sigma_1 = 0.190$ (after Brown and Swanson [16]).

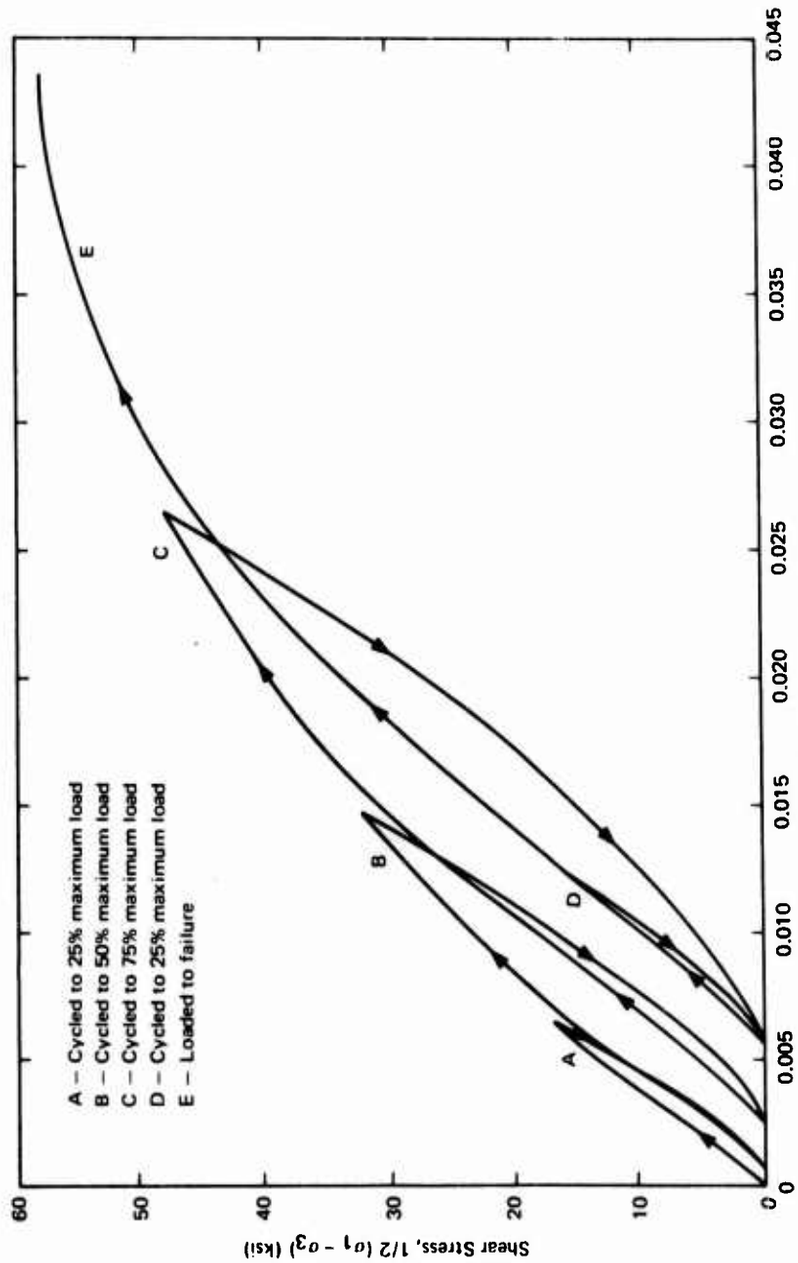

Figure 3. Shear stress–strain curves for Cedar City 6-inch-core granite, specimen no. 18, with $\sigma_3/\sigma_1 = 0.190$ (after Brown and Swanson[16]).

Factors That Influence Behavior

Water. Water may influence the behavior of rock in two ways. First, it may alter the inherent physical properties, usually reducing strength. For instance, Colback and Wiid[14] reported that the strength of saturated quartzitic shale specimens was only about one-half of that for specimens dried over calcium chloride for several weeks. This finding indicates the need for conservative assumptions regarding water content in any analysis where the exact conditions are not known. Second, water under pressure may reduce the strength of porous rocks, such as sandstone, and of brittle rocks with low porosity, such as granite and diabase. In these cases, the law of effective stress used in soil mechanics, as expressed by the following equation, holds:

$$\sigma_{eff} = \sigma_{total} - \sigma_{pore} \qquad (1)$$

where σ_{eff} = effective stress

σ_{total} = total applied stress

σ_{pore} = pore water pressure

In other words, the total stress applied on a rock specimen is equal to the stress in the rock skeleton, σ_{eff}, plus the pore water pressure, σ_{pore}. The strength of a rock specimen is not proportional to the total stress, but is proportional to the effective stress.

The law of effective stress, however, does not hold for limestone and marble under medium to high confining stresses (above about 2.5 kilobars) where these rocks behave as ductile materials. Under confining pressures above 4.5 kilobars, the exterior pores, if any, are sealed off as a result of plastic flow, preventing penetration by water into the interior pores. Significantly, the rate of loading is important in problems where the influence of moisture is dominant. Under static conditions, the load rate is slow enough to permit the pore water pressure to redistribute itself. On the other hand, load rates under blast conditions do not permit pressure redistribution. As a consequence, dynamic pore pressures will build up locally with a resultant lowering of the strength of the rock. This strength reduction must be considered in the design of openings in rock subjected to blast loads.

The law of effective stress also governs the deformation of porous rocks under the influence of pore water pressure, because the deformation of porous media is proportional to the effective stress rather than to the total stress. The effects of pore water pressure on the deformation of low porosity rocks, such as granite, is negligible.

Load Path. Mohr envelopes (strength failure curves) for rocks such as granite, sandstone, and marble, in triaxial compression are independent of the load path.[15,16] That is, the strength of the rock is about the same (within 5 to 10%) whether it is loaded in constant confining pressure, in proportional loading (where the ratio of the confining and axial stress is held constant), or in constant mean stress. An illustration of this behavior for Westerly granite is presented in Figure 4. Dotted lines in this figure represent the load paths used to reach the strength failure envelope.

State of Stress. The strength of a given rock increases with the confining stress or mean stress as shown by the Mohr envelope (solid line) in Figure 4. The amount of inelastic action before strength failure also increases with confining pressure. This effect, however, is less for the stronger rocks than for the weaker ones.

Moreover, the shear stress has a pronounced effect on the volumetric stress-strain behavior of a given rock. In most cases, a specimen bulks under the influence of shear stress. A good example of this behavior may be found in the work by Brown and Swanson.[17] In the study, specimens were first loaded hydrostatically to a given pressure, and then the confining pressure was decreased as the axial stress was increased. The objective was to keep the sum of the three principal stresses, J_1, constant while the shear stress was increased. Mean stress–volumetric strain curves and shear stress–shear strain curves for two sandstone specimens from Brown and Swanson's work are presented in Figures 5 and 6, respectively. The knee of each curve in Figure 5 represents the point at which the shear stress starts to increase; the shear stress causes the specimen to become dilatant. Dilatancy is absent under hydrostatic pressure, as shown by the portion of the curve below the knee. The corresponding shear response of the specimens is shown in Figure 6. From these two figures, it is apparent that dilatancy is associated with shearing stress. Additional work is required to determine (1) the mechanisms that cause coupling between shear stress and dilatancy, and (2) the coupling relation for different rocks.

As with soils, the initial shear modulus of a rock increases with the confining pressure (Figure 7). This effect increases with the rock porosity; the increase in initial shear modulus with confining pressure is slight for a low porosity rock such as granite.

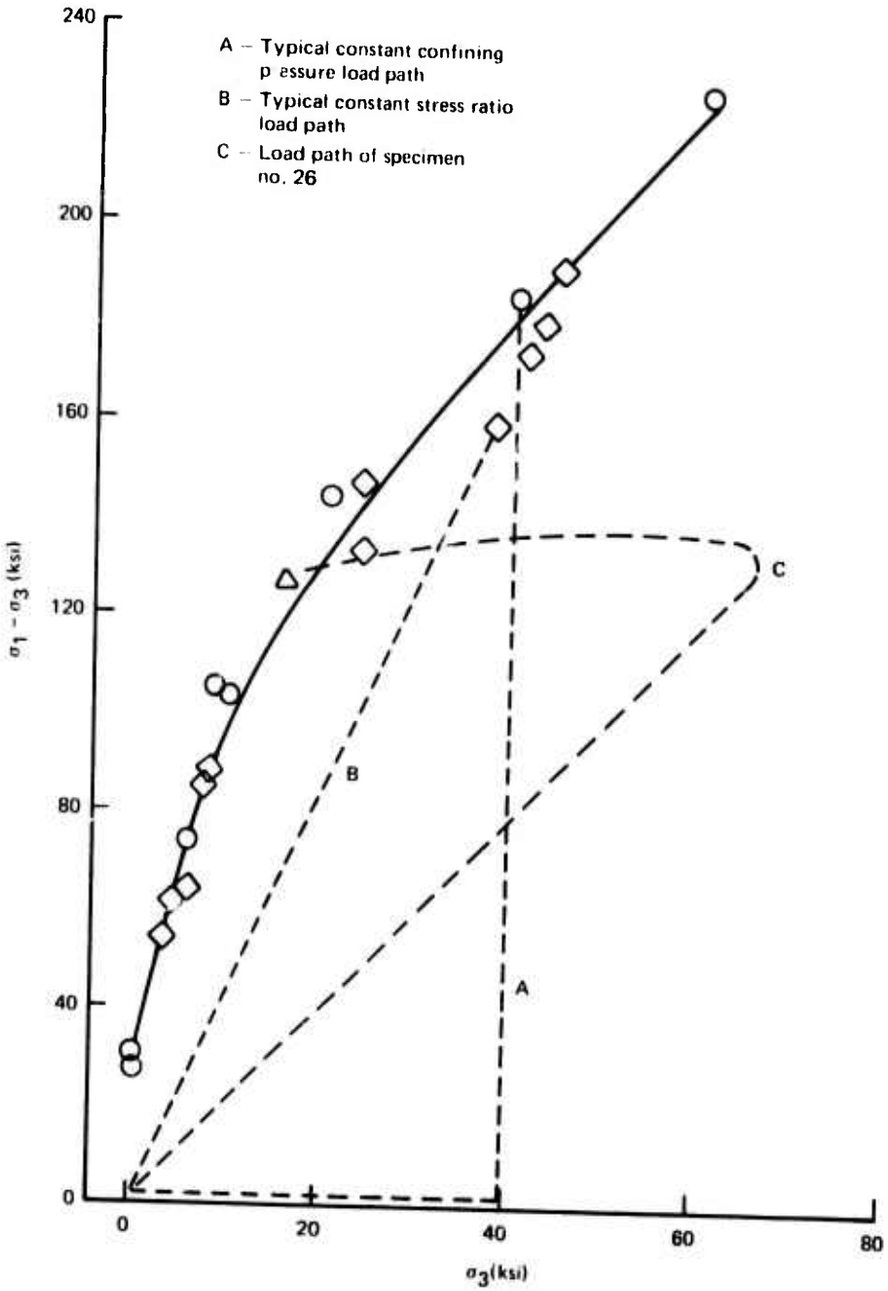

Figure 4. Failure envelope for westerly granite, showing independence of loading path (after Brown and Swanson[15]).

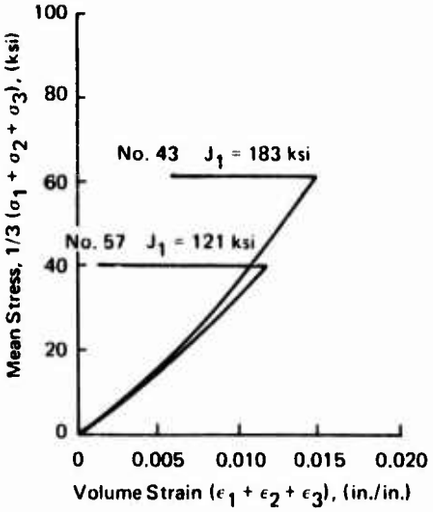

Figure 5. Dilatation stress–strain curves of nugget sandstone in constant J_1 tests (after Brown and Swanson[17]).

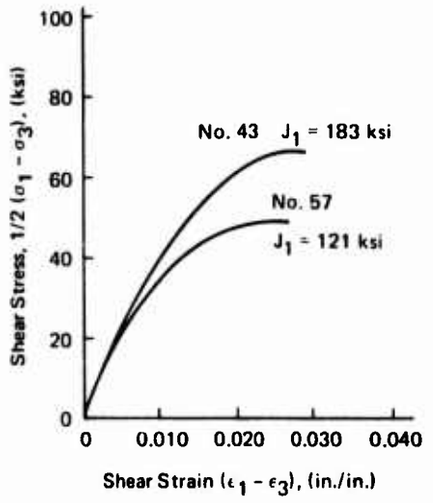

Figure 6. Shear stress–strain curves for nugget sandstone in constant J_1 tests (after Brown and Swanson[17]).

Rate of Loading. As would be expected, the deformation modulus of a rock increases with the rate of loading. Characteristic features of the stress–strain response for rock under high strain rates (2 to 5 x 10^3 in./in./sec) are similar to those seen in low strain rate (10^{-4} in./in./sec) tests.[18, 19] For example, Brown et al.[18] reported a 15 to 20% increase in the modulus for Nugget sandstone when the strain rate was increased from 10^{-4} in./in./sec (static) to 2 to 5 x 10^3 in./in./sec (dynamic). The relative magnitude of the increase in strength of a dry rock is about the same as that for the modulus increase. Under dynamic conditions, the characteristic coupling between shear and volumetric strain is similar to that observed in the static response. Dilatancy also occurs at the higher loading rates. Likewise, the amount of hysteresis and permanent set is comparable with that seen in static tests. On the other hand, the long-term strength (greater than 3 hours) for most rocks is only about 75 to 85% of the corresponding static strength.[9]

One-Dimensional Strain. The behavior of marble, tuff, granite, gabbro, and diabase in one-dimensional strain has been studied experimentally by different investigators.[20-22] In these triaxial tests, the radial expansion of the cylindrical specimen due to axial compression was inhibited by the application of the confining pressure in the radial direction; this process produces a radial contraction

equal to the radial expansion. No failure of the rock specimens was observed by these investigators, but some densification of the more porous specimens was observed. In addition no faults, fractures, or offsets larger than the grain diameter were observed.

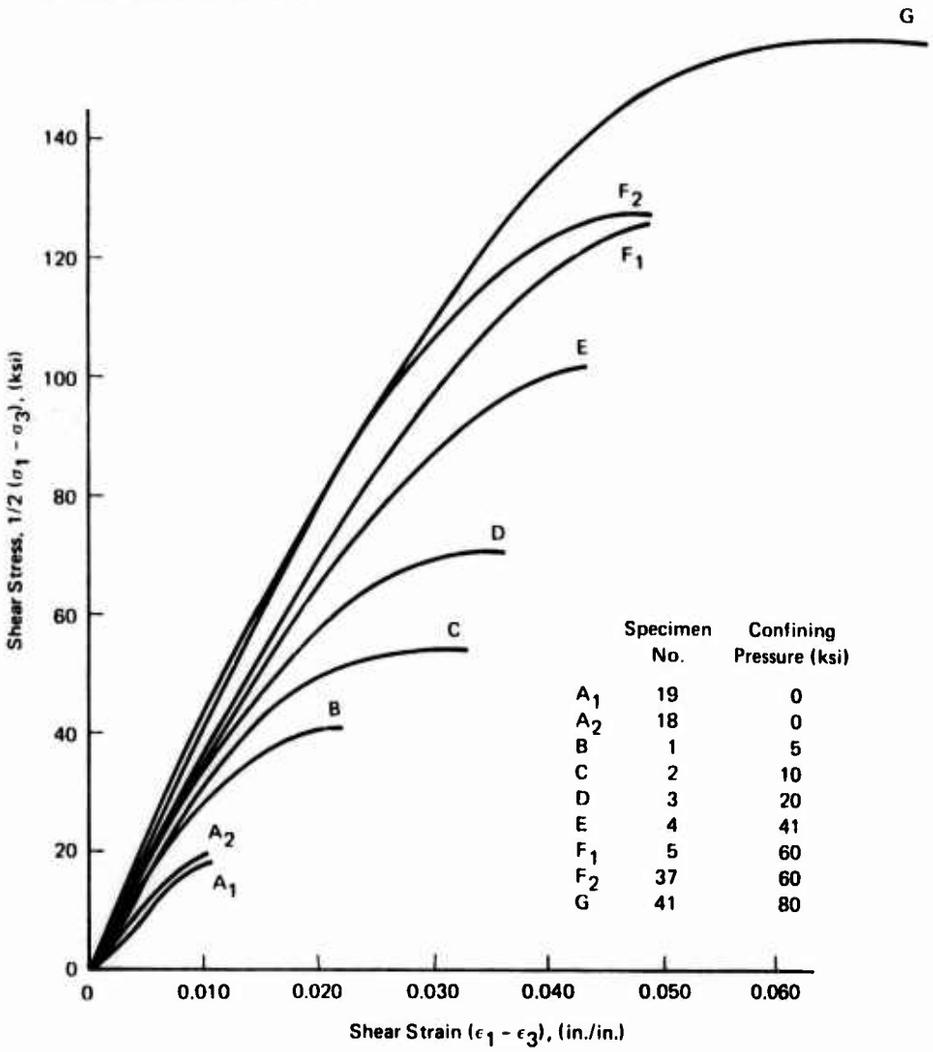

Figure 7. Shear stress–strain curves of nugget sandstone in constant confining pressure tests (after Brown and Swanson[17]).

Rocks that have linear axial stress–axial strain curves show very little permanent volumetric deformation. By contrast, rocks that have a highly nonlinear stress–strain curve (that is, rocks with porosity greater than 2%) show distinct permanent volumetric deformation.[22] The stress loading path of a rock in one-dimensional strain tests is uniquely defined by the strain condition.

The mechanical properties of an intact rock vary with mineral composition, grain size, grain configuration, rate of loading, state of stress, and other factors. Furthermore, on a microscopic scale, intact rocks generally contain cracks randomly distributed along their grain boundaries. Deformation behavior and fracture mechanisms of intact rock under compressive loading are characterized by the growth of cracks and the deformation of the mineral grains. Under low loads, pre-existing cracks in the rock close. This is characterized by the curved axial stress–volumetric strain and axial stress–axial strain curves in Figure 1. Deformation of the mineral grains commences when all the pre-existing cracks are closed. The stress–strain curve for this stage is linear. As the applied load is increased further, stable fracture propagation begins, and pre-existing cracks start to extend. Stable fracture propagation is a function of the load, crack length, and properties of the material and may be stopped in the stable region by holding the load constant. The critical energy release point marks the end of stable fracture propagation (Figure 1).

Unstable fracture propagation starts at loads above the critical energy release point at which the curvature of the axial stress–volumetric strain curve changes sign. Crack growth in the unstable region is governed by factors other than loading such as the crack propagation velocity and the amount of energy stored in the specimen, and, thus, is uncontrollable. At loads above the critical energy release point, the rock becomes dilatant, and the volume of the specimen increases with increasing compressive load. Dilatancy, caused by the opening of axial cracks in the direction of the major principal compressive stress, is associated with shear stresses. The exact relation between dilatancy and shear stress for different rocks is not known at present.

The fracture process for the rock material is concluded when stress failure (maximum strength) is reached. Strength failure, a characteristic property of the rock, defines the transition from a predominantly continuous material to a predominantly discontinuous material. The cracks coalesce, and forking takes place after strength failure, leading to the ultimate rupture of the rock system. Rupture is not a fundamental property of the rock material; rather, it is attributable to the discontinuous rock structure system. Rupture is the overcoming or breaking down of the stability of a fractured rock system.

FRACTURED ROCK

Underground openings, whether lined or unlined, are often surrounded by a ring of rock that is either fractured during the excavation process or by the relief of stresses following formation of the opening. Yet, many unlined

openings remain stable, indicating that fractured rock is still able to carry the load. A good understanding of the deformation behavior of fractured rock is necessary to estimate the contribution of the fractured rock to the strength of lined or unlined openings.

Properties obtained from intact rock specimens are, by themselves, inadequate for defining the behavior of in-situ rock. Because of the presence of discontinuities, the behavior of fractured rock under static loading is markedly different from that of intact rock. The deformation of fractured rock tends to concentrate along major discontinuities. As a consequence, stress wave propagation in fractured rock is also different from that in intact rock.

Literature on the behavior of fractured rock is limited because most of the definitive rock mechanics investigations have been on intact rock, but some information is available from References 11, 18, 23, 24, and 25.

Deformation Behavior in Compression

The general character of the stress–strain behavior of fractured rock in compression is similar to that for intact rock. However, the deformation modulus is much lower, with it decreasing with increasing deformation. Also, hysteresis loops and permanent deformations upon unloading are larger than those for an intact specimen. Initial slope of the shear stress–strain curve increases with confining pressure as observed for the intact specimen, but the increase is more pronounced than that for an intact specimen. A limiting shear stress is reached after which the specimen is strained considerably with a small increase in shear stress. Maximum strains of 20% may be obtained in some cases. The difference between the limiting shear stress of a rock for two different confining pressures is approximately equal to the difference in confining pressure. Mean stress–volumetric strain plots exhibit dilatancy in the same manner as intact specimens, except at much lower stresses. Deformation of an intact specimen is primarily due to the deformation of its constituent grains. By contrast, most of the deformation of a fractured specimen is localized in discontinuities or faults.

Fortunately, fractured rock behaves in a relatively consistent and predictable manner. In his study on the behavior of fractured rock, Bieniawski[11] tested sandstone specimens in uniaxial compression by loading the specimens beyond strength failure in a stiff testing machine and subsequently cycling the specimen in the post-strength-failure range. The fractured specimen was found to unload approximately in a linear path and reload in a similar manner with a very narrow hysteresis loop (Figure 8). Once the previous maximum stress had been reached, the specimen behaved as though it had been subjected to a gradually decreasing load.

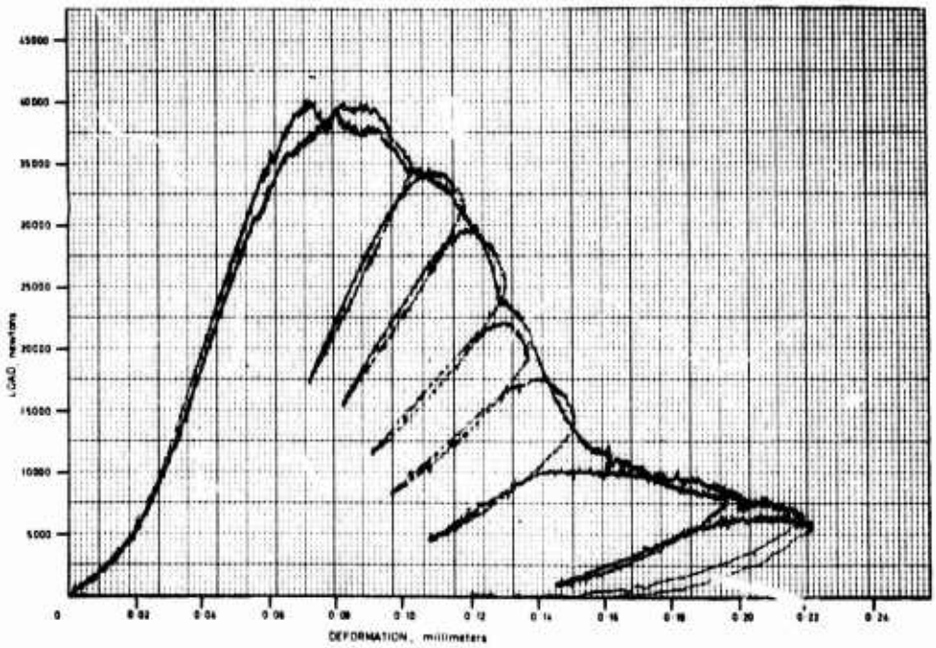

Figure 8. Comparison of deformational behavior of two identical sandstone specimens in uniaxial compression—one subjected to gradually increasing load and the other to cycling load after strength failure. (From Bieniawski.[11]) (Used by permission.)

Factors That Influence Behavior

The strength of a fractured specimen is dependent on the confining pressure. It can be seen from Figure 9 that the strength envelope (dashed line) is approximately parallel to and below the envelope for the intact specimens. A significant point not readily apparent from Figure 9 is that the prefractured specimen retains a major portion of its intact strength. Moreover, fractured rock exhibits time-dependent behavior as intact rock. That is, the strength of the specimen increases with the strain rate, while the opposite occurs with decreasing strain rate.

Information on the influence of water on the behavior of fractured rock may be found in Brown and Swanson's work on granite.[15] They reported that water has very little effect on the strength envelope for fractured granite when the degree of saturation is less than 50%. However, the failure envelope changes drastically at 100% saturation. Under full saturation, rock strength becomes independent of confining pressure and is reduced to essentially the unconfined compressive strength.

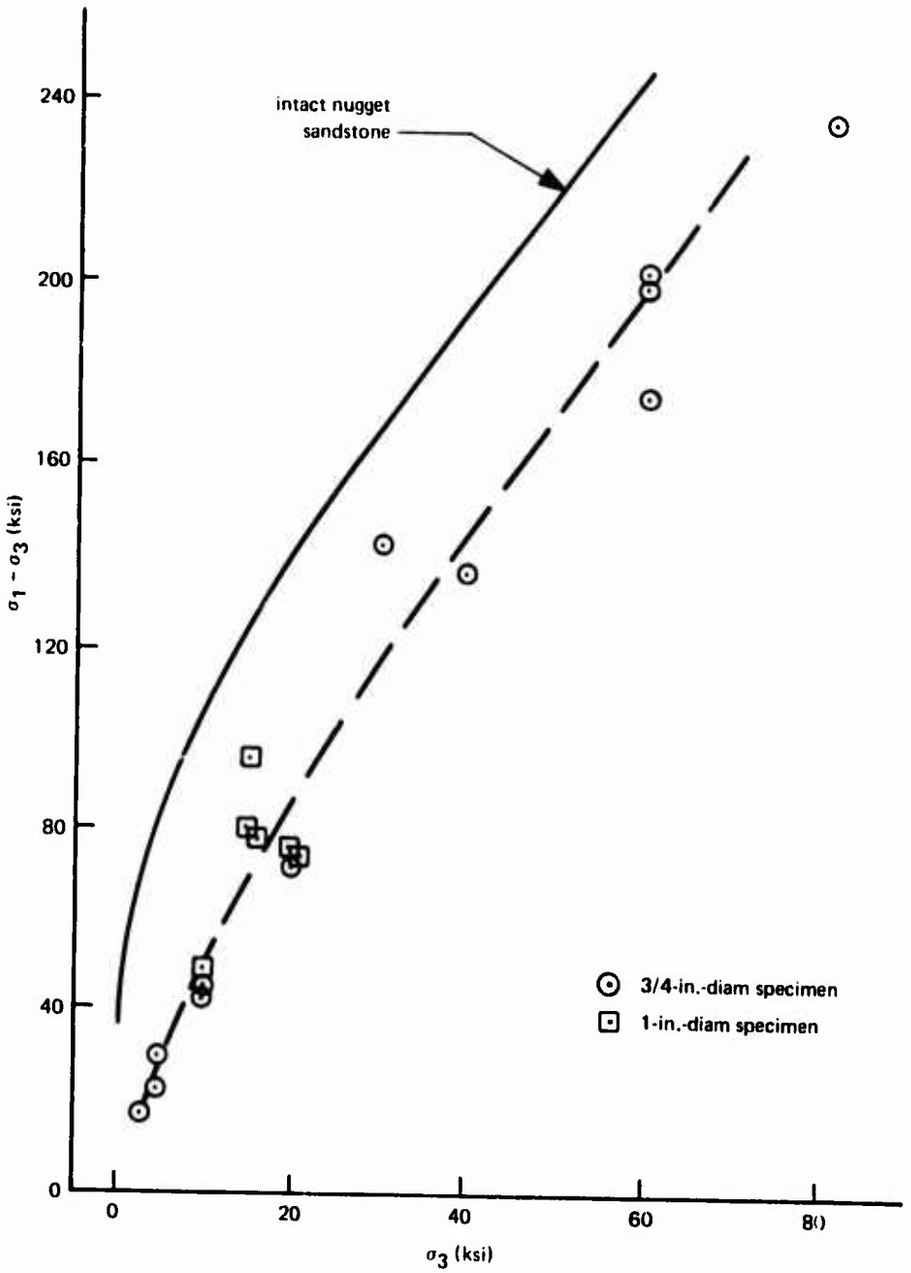

Figure 9. Maximum axial stress difference for prefractured nugget sandstone (after Brown, Swanson, and Wawersik[18]).

A fractured rock specimen can still possess load-carrying ability (strength) after strength failure. Deformation is larger and strength is less than those for the intact material. The practical implication of these observations is that the strength failure of the intact rock material should not govern the design of an opening in rock. Instead, the stability of the structural system (the opening, the liner and backpacking, if any, and the surrounding rock mass) should govern the design.

Since the strength of fractured rock is dependent on the confining pressure (Figure 9), it would seem that the strength of installations in fractured rock might be increased by using a stiff liner together with rock bolts that exert a compressive stress on the surrounding rock. Generally, this is an inefficient and uneconomical solution. Experience in civil tunneling[26] and in weapon effects tests[2] has shown that a better approach is to use a liner or a liner–backpacking arrangement that permits radial deformation and shear adjustment around an opening. With this system, stress redistribution is permitted, vastly reducing liner requirements and generally enhancing the survivability of the system. The liners will prevent damage to equipment from spalls and fly rock, and loose rock from falling into the opening. In addition, liners will enhance the structural integrity of openings in fractured rock.

In some cases, fractured rock continues to deform under constant load. As a consequence, displacement of walls in new rock excavations should be closely monitored to insure the stability of the opening.

Additional work on fractured rock is needed because of the limited knowledge about the quantitative behavior of such rock. Work is required to determine:

1. Stress–strain curves for different types of fractured rock under different static loading conditions.
2. The behavior of fractured rock under cyclic loading.
3. The behavior of fractured rock under dynamic loading, including the influence of water.

JOINTED ROCK

Rock masses generally contain discontinuities such as joints, faults, and bedding planes. These discontinuities have a great influence on the behavior of lined or unlined openings in rock. The strength of an unlined opening in a rock mass, for instance, may be only a few percent of the corresponding strength of an opening in the intact material. In general, the

joints and faults control the survivability of a facility built in a rock mass, because deformation of the rock mass tends to concentrate along these discontinuities. Movement along them may lead to loss of structural integrity. Experimental results from DATEX II[27] showed that block motion in jointed rock could cause the partial or complete cutting off of openings wherever sliding joints intersect structures. Moreover, fallout of loose rock blocks could greatly reduce the strength of an unsupported opening in rock by increasing the effective span of the opening.

At present, little is known about the mechanics of in-situ jointed rock, because a rock system consisting of a large number of joints, each of different length and orientation, is highly indeterminate. As a consequence, most of the knowledge of jointed rock behavior is obtained from laboratory tests on artificial rock. An indication of the probable modes of failure of in-situ rock can be obtained from such tests. In addition, the quantitative influence of parameters, such as joint spacing, orientation, and confining pressure, can be approximated. It is difficult, however, to scale laboratory test results to in-situ situations. Perhaps the most profitable use of laboratory tests on jointed rock models is to provide a check on analytical models, which can then be extended to prototype design and analysis.[4]

Friction Along A Single Joint

Theory. Friction is the resistance to motion caused by the interaction of surface irregularities, called asperities, on two sliding surfaces. Interaction between sliding surfaces is controlled by the contact of asperities and interlocking of asperities.

The contact of asperities and its implications for friction have been treated by Bowden and Tabor.[28] They have shown that asperities on two sliding surfaces are generally not in complete contact with each other, as is indicated schematically in Figure 10. For a ductile solid, the true solid-to-solid contact area is increased because of plastic flow if the normal load is increased, but the normal stress acting on the true contact area remains a constant—the yield strength of the material. This increase in contact area leads to a proportional increase in shear resistance to sliding because the shear stress is a constant during plastic flow. As a consequence, normal force and shear force for ductile materials are interdependent and related by a constant. This constant is called the coefficient of friction, μ; it is defined by Amonton's law: $\mu = \tau/\sigma_n$, where τ is the shear stress and σ_n the normal stress. Shear stresses and normal stresses are obtained from the shear forces and normal forces by dividing each by the apparent area. Understandably, the solid-to-solid contact area will be (at least theoretically) equal to the

apparent area of contact if the normal load reaches a sufficiently high level. Thereafter, the shear stress force will remain a constant, independent of the normal load.

Bowden and Tabor[28] stated that, for brittle materials, the three-dimensional stresses at the tips of asperities can cause plastic flow, which is, in some respects, similar to the friction behavior in ductile material as described above. They presented photographs as evidence of plastic flow in diamonds.

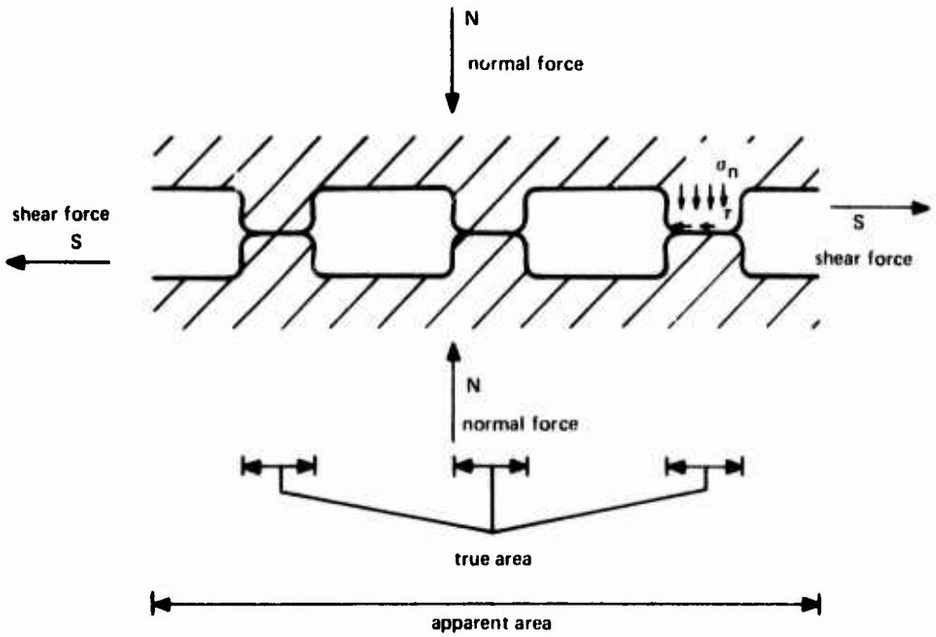

Figure 10. Contact of asperities.

On the other hand, Byerlee[29] states that another friction mechanism may prevail for brittle materials. The tips of asperities crush to a certain extent under the action of the applied normal load. The extent of this crushing is determined by the compressive strength of the material.

When the shear load is applied, additional breakage of asperities takes place because the tensile stress induced at the asperities exceeds the tensile strength. The shear force and normal force for such a material during sliding can be related to the shape of the asperities and to the ratio of the tensile to compressive strength. On the assumption that all shapes of asperities are possible, the applied shear stress and normal stress can be related by the following equation:[29]

$$\frac{\tau}{\sigma_n} = C_1\left(\frac{\sigma_t}{\sigma_c}\right) + C_2 \qquad (2)$$

where τ = shear stress

σ_n = normal stress

C_1, C_2 = constants independent of the material

σ_t/σ_c = ratio of tensile to compressive strength, for example, ≈ 0.1 for rocks

Byerlee[29] based his approach on the assumption that the stress–strain relation for the material is linear to failure. It is unlikely, however, that the asperities will fail in a purely elastic manner even if plastic failure is ruled out. Coefficients of friction computed from Byerlee's formula are generally lower than the range of values found from friction tests on quartz surfaces.

In short, there are at least two different hypotheses on the nature of friction for brittle materials. Bowden and Tabor propounded that some plastic flow occurs at the tips of asperities of two sliding surfaces even for brittle materials. On the other hand, Byerlee[29] analyzed friction for brittle materials on the assumption that the behavior of the asperities is purely elastic. Additional research is required to evaluate these conflicting hypotheses.

Interlocking of asperities is the other factor governing friction. Normally, two sliding surfaces will not be in complete contact with each other. Instead, some small portion will be in solid-to-solid contact as illustrated in Figure 11.

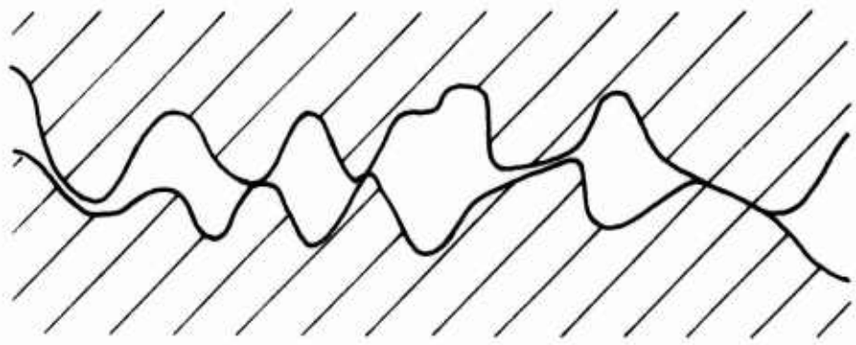

Figure 11. Interlocking of asperities.

Interlocking influences the relation between normal force and shear force for sliding between two surfaces. Dilatancy can occur under small to medium normal forces when the asperities slide over each other (Figure 12b). The shear resistance in this case may be expressed as:

$$S = N \tan(\phi_s + i) \quad (3)$$

where S = shear force

N = normal force

ϕ_s = friction angle for sliding between two surfaces of the same material

i = inclination of the asperity

From Equation 3, it is apparent that the inclination of the asperity causes an increase in shear strength. However, an unfavorable asperity inclination that causes the block to slide downward instead of riding upward (Figure 12b) can reduce the shear strength.

After a pair of asperities have ridden up on each other to a certain level, the stress in the base of the asperity will reach the failure strength and shear off at the base. Under high normal force, the asperity is sheared off at its base before any dilatation occurs because the amount of energy required to shear an asperity is less than that required to ride up the asperity. The relation between shear force and normal force, is then:

$$S = K + N \tan \phi_r \quad (4)$$

where ϕ_r = residual friction angle of the material

K = the ordinate of the intersection of the straight line used to approximate the S–N curve at relatively high normal forces with the shear force axis (Figure 13)

From Figure 12 it is apparent that as the horizontal displacement becomes large, interlocking and the shear strength are reduced. The practical implication of this observation is that supports, when required, should be placed in excavated openings in a jointed rock mass as soon as possible to prevent large sliding movement along joints. This will reduce the probability of instability failure. Large displacements often occur in underground excavations wherein interlocking between the surfaces of rock blocks is lost if supports are not placed properly. The remedial support required to maintain stability is often much greater than the support required to prevent sliding in the first place.

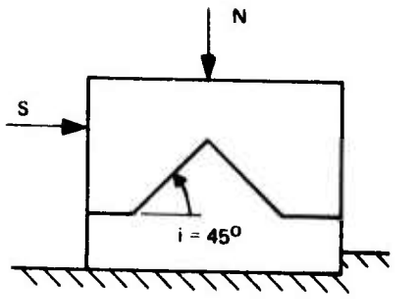

(a) Initial state.

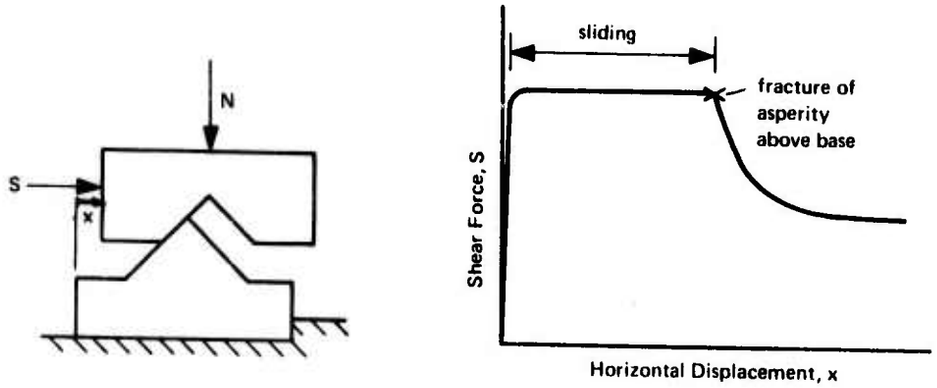

(b) Dilatancy.

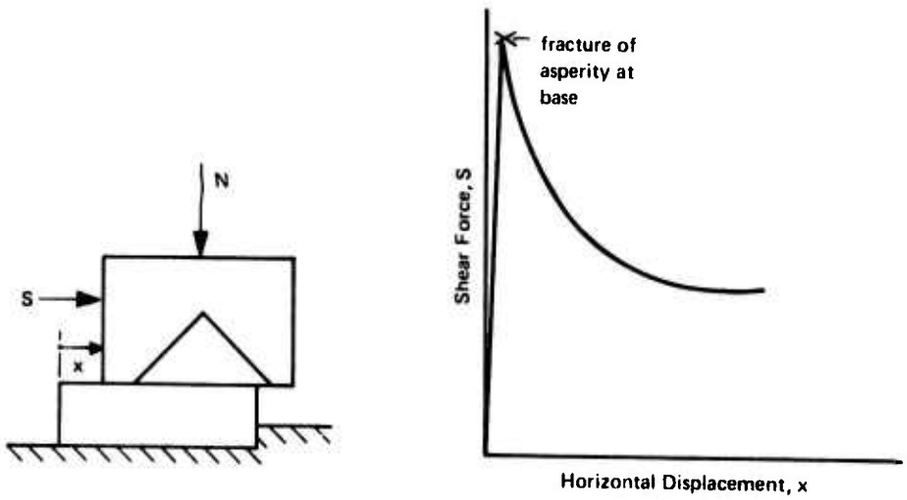

(c) Shearing at base.

Figure 12. Dilatancy and shearing of asperities—scheme of mechanisms and corresponding load–displacement curves.

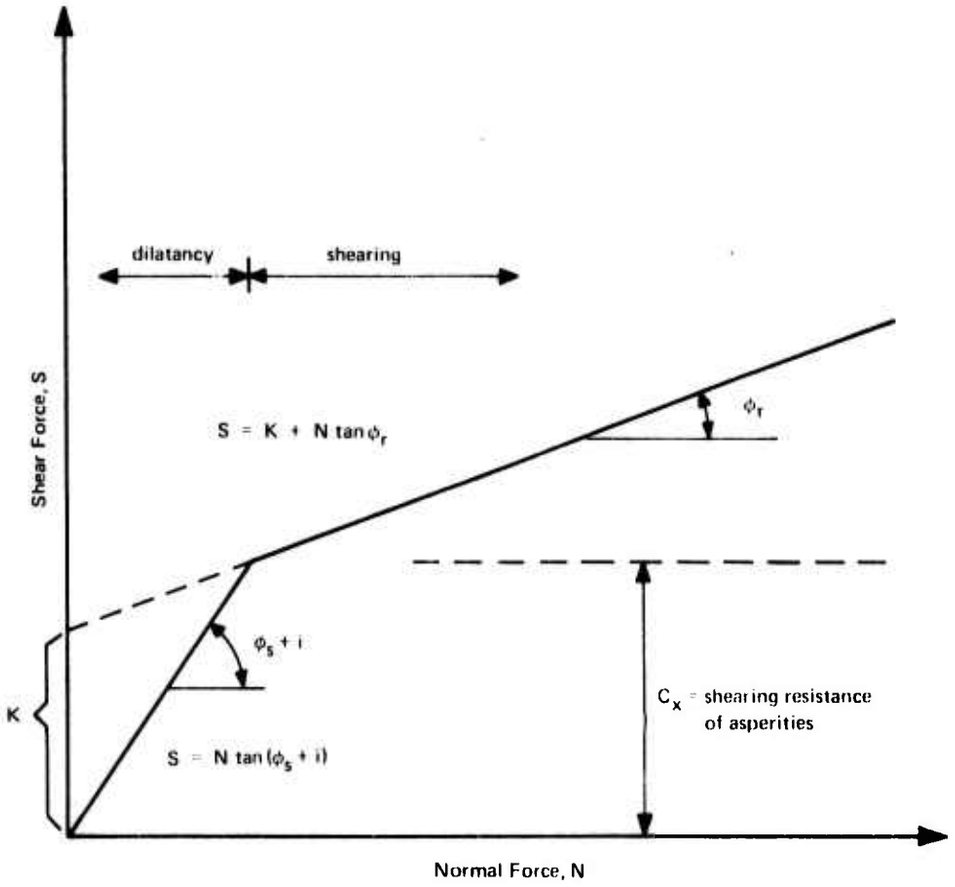

Figure 13. Dilatancy and shearing of asperities—characteristic Mohr envelope.

The influence of interlocking on the shear force–normal force curve has been established by Patton[30] for an artificial material. He showed that the portion of the shear strength envelope below the dashed line, $S = C_x$ is attributed to the shear resistance of the asperities (Figure 13). This shear resistance is governed by the intact strength, number, width of the base, and the inclination of the asperities.

The Mohr friction envelope for most rocks will not have the bilinear shape shown in Figure 13, but will have the initially curved shape shown in Figure 14. This is because the asperities of rocks have different heights and shapes, causing a mixture of dilatancy and shearing in the relatively low normal force range.

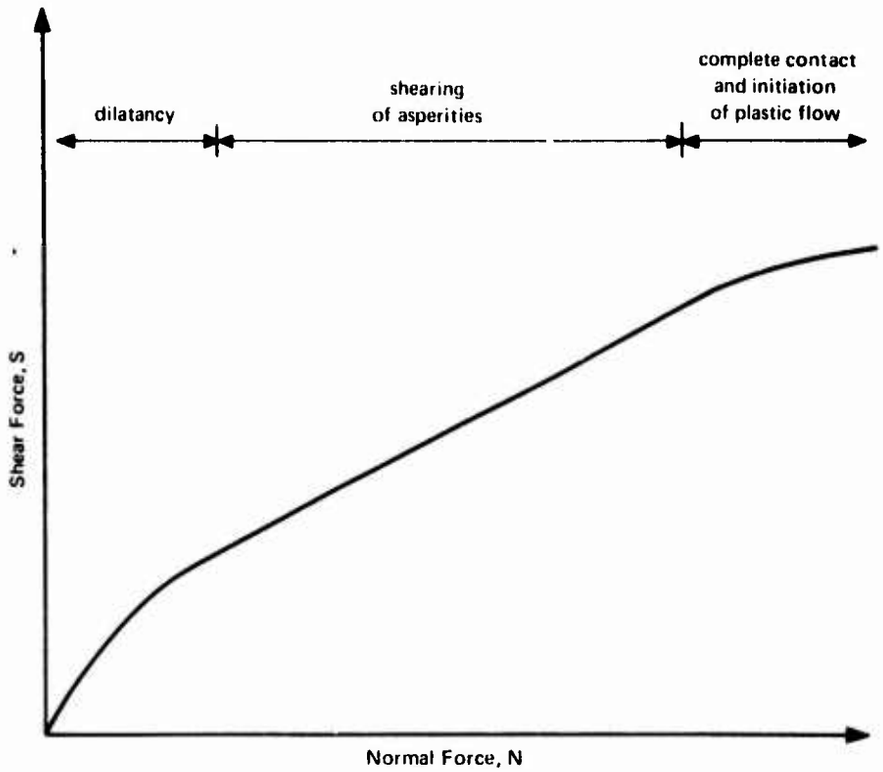

Figure 14. Mohr envelope for the entire range of friction.

In sum, contact and interlocking of asperities determine the relation between the shear force and the normal force for two sliding surfaces. This relationship, illustrated in Figure 14, corresponds to a sequence of three mechanisms:

1. Dilatancy under small normal forces (the initially curved portion)
2. Shearing of asperities at their bases under intermediate normal forces (the straight-line portion)
3. Complete contact of surfaces with plastic flow under high normal forces (the final curved portion)

The last portion of the curve is of little interest in the analysis of underground openings, because normal stresses in the rock joints in the vicinity of an opening will be relatively low.

Friction Behavior of Rock. The friction behavior of rock has been examined by many investigators, principally with direct shear and triaxial tests. A composite of data defining the Mohr envelopes for various ductile

and brittle rock is presented in Figure 15.[31] Remarkably, the data lie close to a common envelope, which has an initially curved portion. Patton's tests[30] on an artificial material indicated that dilatancy is largely responsible for the initially curved portion of the friction envelope. This fact is confirmed by Byerlee[29] who reported that the coefficient of friction is linear (that is, the envelope is linear and passes through the origin) for rough granite sliding on sapphire in which no dilatancy occurred.

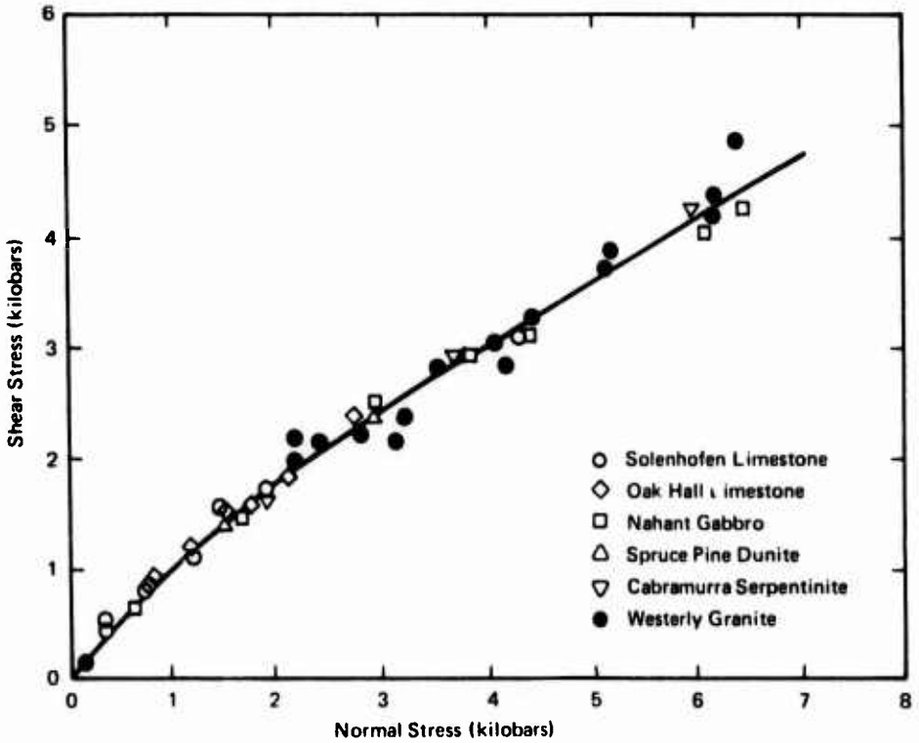

Figure 15. Mohr envelope for friction of different rocks (from Byerlee[31]).

Bromwell[32] found considerable difference in the coefficient of friction for quartz, depending on the surface roughness and cleanliness. He reported that the friction coefficient was about 0.1 for smooth, oil-contaminated surfaces and between 0.3 and 0.8 for rough, clean surfaces. Conceivably, friction coefficients of other rocks are also governed by their surface roughness and cleanliness. The fact that the Mohr friction envelopes for most rocks have similar characteristics but different coefficients of friction leads to the following conclusions:

1. The microscopic roughness that determines residual surface friction (after large displacements) is similar for most rocks.

2. Surface roughness has much less effect on the coefficient of friction for contaminated surfaces than for clean surfaces. The effect of surface roughness tends to be masked by the contaminant.

3. Macroscopic roughness is related to the strength of the intact material. That is, sharp asperities are found on surfaces of high-strength materials and smooth asperities are found on low-strength materials. As a result, the force required to shear both types of asperities is about the same.

Influence of Water. The shear resistance of a joint increases with the effective normal stress in the asperities. Water under pressure reduces the effective normal stress. Hence, pore water under pressure may greatly reduce the shear resistance of a joint. In addition, water alters the deformation behavior and reduces the strength of filled joints by changing the properties of the filling material. The properties of filling materials, such as clay or rock flour, are adversely affected by the presence of water. It follows that saturation should be assumed for filled joints in wet sites when performing the stability analysis of openings in rock in order to prevent catastrophic failures.

Nature of Rock Joints

Origin. Joints in rock masses originate from breakage of the intact material under tension or shear forces. Surfaces of extension joints are rough; by contrast, surfaces of shear joints are smooth. The latter joints generally contain fillings of clay, gouge, or crushed rock. In geology terminology, joints with shear features are classified as faults, but they will be given a special denotation in the following discussion.

Types of Joints. The rock joint classification used here was adopted from Goodman's work.[5] Accordingly, rock joints are separated into four types, depending on the characteristic of the joint surfaces and the filling material between them.

1. Healed joints and incipient fractures. The shear stress–deformation curve for these joints rises steeply to a peak stress and then quickly falls to a residual value that may be one-third less than the peak value (Figure 16a).

2. Clean, smooth joints. These are artificial joints formed by diamond saw cutting through rock specimens or by grinding and polishing rock specimens. Shear stress–deformation curves for this group (Figure 16b)

also develop the maximum stress at small deformations, but do not fall sharply to the residual strength; rather, the maximum strength is slightly above the residual value. This type of joint rarely exists in nature and is only of academic interest.

3. Clean, rough joints. The shear stress–deformation curve for this type of joint shows a lower stiffness when compared to types 1 and 2. It has numerous secondary peaks (as shown in Figure 16c) which are caused by the overriding and shearing of asperities.

4. Shear zones, clay-filled joints, and smooth bedding and shale partings. The behavior of this type of joints is influenced significantly by a change in moisture content, as illustrated in Figure 16d. At low moisture contents, the shear stress–deformation curve shows a high stiffness and a great difference between peak and residual stresses although it is not as severe as with healed joints. When saturated, the stiffness of such joints is greatly reduced. Joints with saturated, thin seams show strain hardening behavior with the ultimate strength being much higher than the proportional limit. Joints with saturated, thick seams have an elasto-plastic type of shear stress–deformation curve.

In the first three of the above classes, water has very little influence on their behavior.

Deformation Behavior

The deformation behavior of a rock joint is governed by its unit stiffness in compression and in shear, and by its shear strength. Normal stiffness of a joint, k_n, depends on:

1. The solid-to-solid contact area between the two joint surfaces
2. The configuration of the aperture space between the asperities
3. The relevant properties of the filling material

Shear stiffness, k_s, depends on:

1. The roughness of the joint surfaces as determined by the distribution, amplitude, and inclination of the asperities
2. The configuration of the aperture space between the asperities
3. The relevant properties of the filling material

Shear strength of a joint, **S**, depends on:

1. The friction characteristics along the joint
2. The strength of the filling material

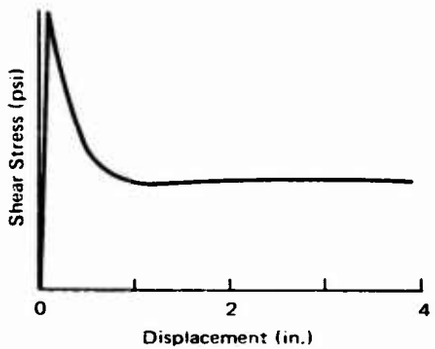

(a) Type 1 – healed and incipient joints.

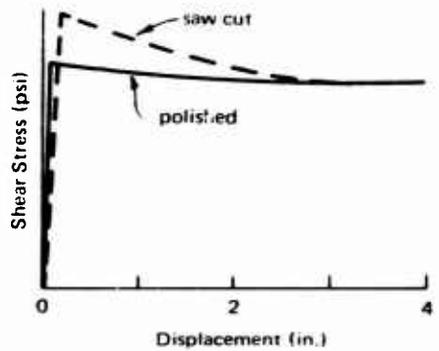

(b) Type 2 – clean, smooth fractures.

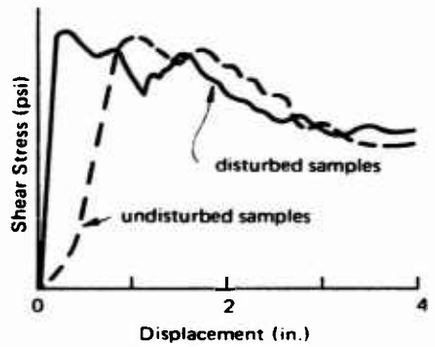

(c) Type 3 – clean, rough fractures.

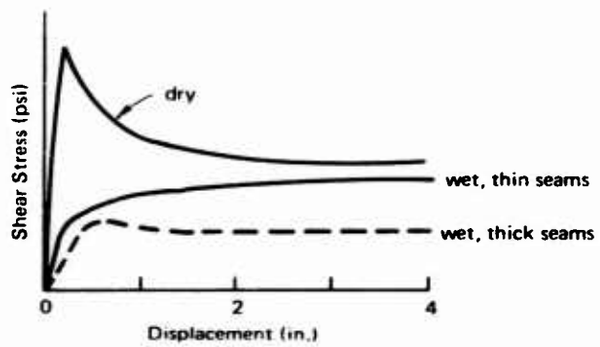

(d) Type 4 – filled joints, sheared zones, and shale partings.

NOTE: Strength depends on the normal stress on the joint surfaces; shear stress scale relative only.

Figure 16. Typical shear stress–deformation relation for different joint surfaces.

Joint strength is independent of its stiffnesses, k_n and k_s. As has been pointed out, the strength of an unfilled joint is primarily dependent on the characteristics of the joint surfaces. By contrast, the shear and normal stiffnesses depend on the configuration of the intervening space between the surfaces and on the properties of the materials occupying that space. The tensile strength of a joint is negligible. Furthermore, filling material between the joint surfaces can have a significant effect on the parameters k_n, k_s, and **S**. Clayey filling, for example, will generally indicate low values of k_n and k_s. In addition, clayey fillings will indicate a low shear strength, except in special cases where extensive interlocking of strong rock asperities dominate the behavior. A well cemented joint, by contrast, may have properties as good as or even better than those of the intact material.

Moisture influences the values of k_n, k_s, and **S** of a filled joint through its effect on the filling material properties. In unfilled joints, moisture affects the joint parameters by reducing the normal stress on the joint according to the effective stress principle discussed earlier.

The individual factors influencing joint parameters k_n, k_s, and **S** are difficult to determine by other than direct measurements. Their determination for different types of rock joints is highly recommended, because they are part of the input data required for finite element analyses of openings in jointed rock masses.

BEHAVIOR OF A JOINTED MATERIAL

Presently, there is no reliable theory that can predict the deformation behavior and strength of a complex, jointed rock mass. Consequently, most of the available knowledge on the subject comes from laboratory studies on jointed-block models made from artificial materials, such as gypsum. Real rock is not ordinarily used in block model studies because of the cost and difficulty in machining specimens. Some of the more recent laboratory studies on the subject can be found in References 33 through 36. Understandably, it is difficult to apply the laboratory test results directly to computing the behavior of natural rock masses. However, these test results are useful in providing an insight into the deformation behavior and failure mechanisms of rock masses in the field.

Deformation Behavior

In most instances, stress–deformation behavior of the most simple jointed model is markedly different from that of the intact material. Deformation of the joints tends to dominate the overall deformation of the model,

because deformation of the intact material is relatively small when compared to the deformation along the joints. The behavior of a jointed model depends on:

1. The strength of the intact material
2. The sliding characteristics of the joint surfaces
3. The inclination of the joint sets with respect to the principal stress direction
4. The joint spacing
5. The boundary stresses

The response of a jointed material under an imposed load is as follows. Initially, slip takes place along the joints. Slip continues as the load is increased until interlocking of the blocks starts, causing high stress concentrations within the blocks and along their boundaries. The stress concentrations due to interlocking increase with the applied load, leading to ultimate failure of the jointed-block system.

Typical stress–strain plots from Brown's study[34] on gypsum block models (Figure 17) are presented to illustrate the characteristic deformation of a jointed material. The model shown in Figure 17 was fabricated from 4-inch-long hexagonal blocks and was subsequently subjected to triaxial load tests. Its overall dimensions were 4 x 4 x 8 inches. From the stress difference–axial strain curves, it is apparent that stick–slip oscillations are present in all the curves except that carried out at zero confining pressure. These oscillations were probably caused by the interaction of the specimen with the testing machine during the overriding and shearing of the asperities along the joints and fracture surfaces.

The specimen tested at zero confining pressure had virtually no residual strength. Samples tested under confining pressures developed considerable residual strength during post peak sliding along joints and/or along fracture planes. The strength of the specimen increases with confining pressure as shown in Figure 17.

It is also apparent from the curves in Figure 17 that the gypsum block model behaved in a ductile manner at confining stresses above 200 psi; below 200 psi, the model behaved in a brittle manner. Furthermore, the deformation modulus of the model increased with confining pressure as observed for fractured rock. The modulus of the jointed model was about one-third to one-half of that for the intact material, except in the unconfined case, where the difference was even more marked. On these curves, there is a general absence of the bedding down region from joint closure as expected for natural rock masses.

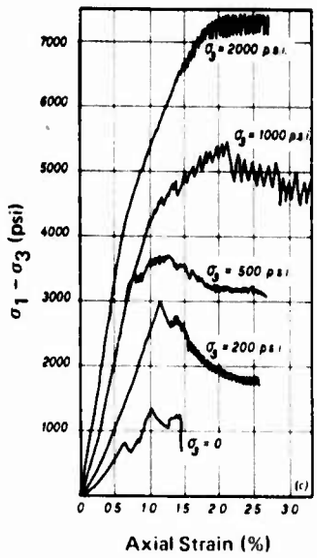

17a

From "Strength of Models of Rock With Intermittent Joints," by Edwin T. Brown, Journal of the Soil Mechanics and Foundations Division, Proceedings of the American Society of Civil Engineers, vol. 96, no. SM6, November 1970, page 1941.

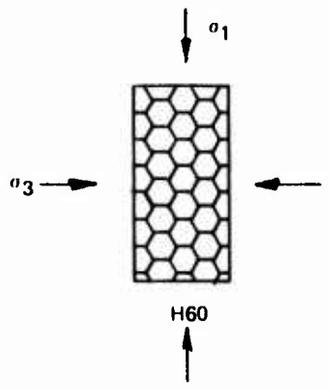

model configuration

17b

Figure 17. Principal stress difference versus axial strain curves for gypsum block model (© American Society of Civil Engineers, 1970.[34] Used by permission.).

In the field, the minor principal stress in the rock surrounding an opening in a rock field is zero or nearly so. Supports are often used to strengthen and enhance the stability of the opening. However, the increase in strength and in modulus of deformation of the rock in the vicinity of the opening due to the supports is negligible. The primary function of the supports is to maintain the integrity of the opening by restraining loosened rock from falling, thereby increasing the effective span of the opening. Note that the strength of a jointed material is much less than the corresponding intact material, except when the jointed material is subjected to relatively high confining pressures. Under high confining pressure, the strength of the jointed material approaches that of the intact material. An illustration of the strength variation of a jointed material with confining pressure is presented in Figure 18.

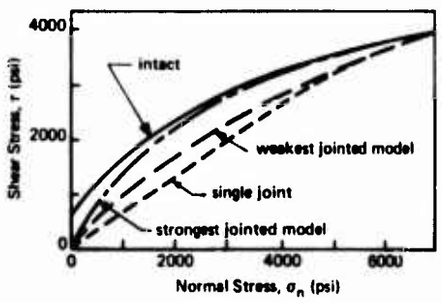

Figure 18. Comparison of Mohr envelopes.

The unloading and reloading curve for the jointed model before and after the peak stress can be represented by a straight vertical line in the stress–strain curve, indicating that none of the axial strain undergone by the specimen is recoverable.

This leads one to conclude that the greater part of the observed strain is from movement along joints rather than from deformation of the intact material within the individual blocks. It follows that the spacing *and* orientation of a jointed mass can have a great influence on its deformation behavior.

In his geomechanical study of a jointed rock model, Rosenblad[35] reported large variations in principal strain magnitudes and directions within a single block and from block to block under uniform stress. Conceivably, the state of strain within each intact block in a jointed material is very complex, depending on the boundary stresses.

Modes of Failure

The failure mode of a jointed material is controlled by the same factors that influence its deformation behavior, namely, the strength of the intact material, the sliding characteristics of the joints, and the inclination of the joint sets with respect to the major principal stress direction, joint spacing, and applied boundary stresses. The following modes of failure are possible for a jointed material:

1. Collapse at low confining pressures as a result of block movements involving the movement of joints, sliding along joints, and dilatation of the specimen.
2. Axial cleavage at low confining pressures.
3. Shear failure of the intact material along an approximately planar surface, independent of joints at low to intermediate confining pressures.
4. Formation of a single composite shear plane, partly through the intact material and partly along joints at low to intermediate confining pressures.
5. Plastic flow or formation of multiple shear surfaces under high confining pressures.

At present, the mechanisms that cause each of the above failure modes are not known. Failure modes 1 and 2 could have practical consequences on the stability of unlined openings in a rock mass.

Hypothetically, the stress–deformation behavior of natural rock masses depends on the same parameters as the aforementioned models. Presently, there is no established theory that can predict the deformation behavior and strength of a jointed rock mass.

FINDINGS AND CONCLUSIONS

The purpose of this study was to review the deformation behavior and fracture mechanisms of rocks. The ultimate goal is to incorporate this knowledge into the development of a nonlinear finite element computer program for analyzing the behavior of lined or unlined openings in a rock mass under static or dynamic loading. From this study it is concluded that:

1. The mechanical properties of an intact rock are not unique. These properties vary with the rock's mineral composition, grain size, grain configuration, state of stress, and strain rate.

2. The deformation behavior and fracture mechanisms of an intact rock are characterized by crack growth and by the deformation of the constituent grains.

3. Dilatancy of rock under compression is associated with shear stress. Dilatancy is not suppressed at the higher loading rates. At present, the mechanisms which cause coupling between shear stress and dilatancy are not known with certainty.

4. Fractured rock can still carry load. However, its deformation modulus decreases with increasing deformation.

5. The deformation of a fractured rock specimen tends to concentrate along the major discontinuities.

6. The deformation of a rock joint is governed by the shear force and normal force on the joint and by the normal stiffness, shear stiffness, and shear strength of the joint.

7. The deformation of a jointed material is dependent on:

   a. The strength of the intact material

   b. The sliding characteristics of the joint surfaces

   c. The inclination of the joint sets with respect to the principal stress direction

   d. The joint spacing

   e. The boundary stresses applied

8. The deformation of a jointed material is characterized by slip along joints, interlocking of the intact blocks, and fracturing of the intact blocks.

9. Under a given state of stress, the stiffness and strength of a fractured or jointed rock are generally lower than those for the intact rock.

The following information is required for a good finite element representation of an opening in a rock mass:

1. Configuration of the opening and major discontinuities, such as joints.

2. Location and extent of fractured rock zones in the vicinity of the opening.

3. Pertinent stress–strain properties of the intact rock, the fractured rock, and the liner, if any.

4. Stress–deformation properties of the major discontinuities.

ACKNOWLEDGMENTS

Messrs. J. R. Allgood, R. M. Murtha, and R. J. Odello reviewed the manuscript and made many helpful suggestions.

REFERENCES

1. Cording, E. J. (1968). The stability during construction of three large underground openings in rock, Army Engineer Waterways Experiment Station, Technical Report No. 1-813, Vicksburg, Miss., Jan. 1968.

2. Classified reference.

3. De Rouvray, A., et al. (1971). Research on rock bolt reinforcement: Analysis and model studies of underground openings in jointed rock, Army Corps of Engineers, Omaha District, Technical Report No. 7, Omaha, Neb., June 1971. (AD 727655)

4. Zienkiewicz, O. C. (1971). The finite element method in engineering science, 2d ed. New York, McGraw-Hill, 1971.

5. Goodman, R. E. (1968). Research on rock bolt reinforcement: Effects of joints on the strength of tunnels, Army Corps of Engineers, Omaha District, Technical Report No. 5, Omaha, Neb., Sept. 1968.

6. Zienkiewicz, O. C. (1968). "Continuum mechanics as an approach to rock mass problems," in Rock mechanics in engineering practice, edited by K. C. Stagg and O. C. Zienkiewicz. New York, Wiley, 1968, pp. 237-273.

7. Zienkiewicz, O. C., et al. (1970). "Analysis of non-linear problems in rock mechanics with particular reference to jointed rock systems," in Proceedings of the 2nd Congress of the International Society for Rock Mechanics, Belgrade, 21-26 Sep. 1970, v.3. Belgrade, Yogoslavia, "Jaroslav Černi" Institute for Development of Water Resources, 1970, pp. 501-509.

8. Brace, W. F. and Byerlee, J. D. (1967). "Recent experimental studies of brittle fracture of rocks," in Failure and breakage of rock; proceedings of the 8th Symposium on Rock Mechanics, Univ. of Minnesota, Sep. 15-17, 1966, edited by C. Fairhurst. New York, American Institute of Mining, Metallurgical and Petroleum Engineers, 1967, pp. 58-81.

9. Bieniawski, Z. T. (1967). Mechanism of brittle fracture of rock, Council for Scientific and Industrial Research, Report MEG-580, Pretoria, South Africa, Aug. 1967.

10. Brace, W. F., Paulding, B. W., and Scholz, C. (1966). "Dilatancy in the fracture of crystalline rocks," Journal of Geophysical Research, vol. 71, no. 16, Aug. 15, 1966, pp. 3939-3953.

11. Bieniawski, Z. T. (1969). Deformational behaviour of fractured rock under multiaxial compression, Council for Scientific and Industrial Research, Report MEG-274, Pretoria, South Africa, 1969. (Also published in: Structure, solid mechanics and engineering design; proceedings of the Southampton 1969 Civil Engineering Materials Conference edited by M. Te'eni, New York, Wiley, 1971, pt.1, pp. 589-598.

12. Brace, W. F. and Orange, A. S. (1968). "Electrical resistivity changes in saturated rocks during fracture and frictional sliding," Journal of Geophysical Research, vol. 73, no. 4, Feb. 15, 1968, pp. 1433-1445.

13. Brace, W. F. and Orange, A. S. (1968). "Further studies of the effects of pressure on electrical resistivity of rocks," Journal of Geophysical Research, vol. 73, no. 16, Aug. 15, 1968, pp. 5407-5420.

14. Colback, P.S.B. and Wiid, B. L. (1965). "The influence of moisture content on the compressive strength of rocks," in Proceedings of the 3rd Canadian Rock Mechanics Symposium, Univ. of Toronto, Jan. 15-16, 1965. Ottawa, Canada, Dept. of Mines and Technical Surveys, 1965, pp. 65-83.

15. Brown, W. S. and Swanson, S. R. (1970). Constitutive equations for Westerly granite and Cedar City tonalite for a variety of loading conditions, Defense Atomic Support Agency, Report No. DASA 2473, Washington, D. C., Mar. 1970. (Contract DASA-01-69-C-0034) (AD 710820)

16. Brown, W. S. and Swanson, S. R. (1971). Influence of load path and state of stress on failure strength and stress-strain properties of rocks, Air Force Weapons Laboratory, Technical Report No. AFWL-TR-70-53, Kirtland Air Force, N.M., Jan. 1971.

17. Brown, W. S. and Swanson, S. R. (1971). Stress-strain and fracture properties of Nugget sandstone, Air Force Weapons Laboratory, Technical Report No. AFWL-TR-71-54, Kirtland Air Force Base, N.M., Oct. 1971.

18. Brown, W. S. et al. (1971). Influence of dynamic loading, biaxial loading, and pre-fracturing on the stress-strain and fracture characteristics of rocks, Defense Atomic Support Agency, Report No. DASA-2713, Washington, D. C., Mar. 1971.

19. Friedman, M. (1970). "Observation of brittle-deformation features at the maximum stress of Westerly granite and Solenhofen limestone," International Journal of Rock Mechanics and Mining Sciences, vol. 7, no. 3, May 1970, pp. 297-306.

20. Brown, W. S., DeVries, K. L., and Smith, S. L. (1967). Properties of rocks tested in one-dimensional compression, Air Force Weapons Laboratory, Technical Report No. AFWL-TR-66-124, Kirtland Air Force Base, N.M., Jan. 1967.

21. Brace, W. F. and Riley, D. K. (1971). Static uniaxial deformation of 15 rocks, Defense Atomic Support Agency, Report No. DASA-2657, Washington, D. C., May 1971.

22. Brace, W. F. and Walsh, J. B. (1971). Elasticity of rock in uniaxial strain, Defense Atomic Support Agency, Report No. DASA-2655, Washington, D. C., May 1971.

23. Swanson, S. R. (1971). Representation of the post-fracture mechanical behavior of Nugget sandstone, Defense Atomic Support Agency, Report No. DASA-2721, Washington, D. C., Mar. 1971.

24. Bieniawski, Z. T. and Denkhaus, H. G. (1969). "Failure of fractured rock," International Journal of Rock Mechanics and Mining Sciences, vol. 6, no. 3, May 1969, pp. 323-341.

25. Crouch, S. L. (1972). "A note on post failure stress-strain path dependence of Norite," International Journal of Rock Mechanics and Mining Sciences, vol. 9, no. 2, Mar. 1972, pp. 197-204.

26. Nussbaum, H. (1972). "Recent development of the new Australian tunneling method," paper presented at ASCE National Structural Engineering meeting, Cleveland, Ohio, Apr. 24-28, 1972. (Preprint 1658)

27. Blouin, S. E. (1970). Data Report, DATEX II, Air Force Weapons Laboratory, Technical Report No. AFWL-TR-69-149, Kirtland Air Force Base, N.M., Jan. 1970.

28. Bowden, F. P. and Tabor, D. (1967). Friction and lubrication. London, Methuen, 1967.

29. Byerlee, J. D. (1967). "Theory of friction based on brittle fracture," Journal of Applied Physics, vol. 38, no. 7, June 1967, pp. 2928-2934.

30. Patton, F. D. (1966). Multiple modes of shear failure in rock and related materials, Ph D. Thesis, Univ. of Illinois, Urbana, Ill., 1966.

31. Byerlee, J. D. (1968). "Brittle-ductile transition in rocks," Journal of Geophysical Research, vol. 73, no. 14, July 15, 1968, pp. 4741-4750.

32. Bromwell, L. G. (1966). Research in earth physics, phase report no. 7. The friction of quartz in high vacuum, Army Waterways Experiment Station, Contract Report No. CR-3-101-7, Vicksburg, Miss., May 1966.

33. Brown, E. T. and Trollope, D. H. (1970). "Strength of a model of jointed rock," American Society of Civil Engineers, Journal of the Soil Mechanics and Foundations Division, vol. 96, no. SM2, Mar. 1970, pp. 685-704.

34. Brown, E. T. (1970). "Strength of models of rock with intermittent joints," American Society of Civil Engineers, Journal of the Soil Mechanics and Foundations Division, vol. 96, no. SM6, Nov. 1970, pp. 1935-1949.

35. Rosenblad, J. L. (1971). "Geomechanical model study of the failure modes of jointed rock masses," Army Corps of Engineers, Missouri River Division, Technical Report No. 1-71, Omaha, Nebraska, Jan. 1971.

36. Einstein, H. H., Bruhn, R. W. and Hirschfeld, R. C. (1970). Mechanics of jointed rock; experimental and theoretical studies, Interim report R70-62, Massachusetts Institute of Technology, Dept. of Civil Engineering, Cambridge, Mass., Aug. 1970. (PB 195917)

LIST OF SYMBOLS

C_x	The portion of the shear strength of a joint attributed to the shear resistance of the asperities
C_1, C_2	Constants
i	Inclination of the asperity
J_1	Sum of three principal stresses
K	The ordinate of the intersection of the straight line used to approximate the S–N curve at relatively high normal forces with the shear force axis
k_n	Normal stiffness of a joint
k_s	Shear stiffness of a joint
N	Normal force
S	Shear force, or shear resistance
x	Horizontal displacement
$\epsilon_1, \epsilon_2, \epsilon_3$	Principal strains
σ_c	Compressive strength
σ_{eff}	Effective stress
σ_n	Normal stress
σ_{pore}	Pore water pressure
σ_t	Tensile strength
σ_{total}	Total stress
$\sigma_1, \sigma_2, \sigma_3$	Principal stresses
ϕ_r	Residual friction angle of the material
ϕ_s	Friction angle for sliding between two surfaces of the same material
τ	Shear stress
μ	Coefficient of friction